Supplementary material for the paper

Effects of dust aerosols on tropospheric chemistry during a typical pre-monsoon season dust storm in northern India

Rajesh Kumar[1, 2], M. C. Barth[2], S. Madronich[2], M. Naja[3], G. R. Carmichael[4], G. G. Pfister[2], C. Knote[2], G. P. Brasseur[1, 5], N. Ojha[3] and T. Sarangi[3]

[1]Advanced Study Program, National Center for Atmospheric Research, Boulder, USA

[2]Atmospheric Chemistry Division, National Center for Atmospheric Research, Boulder, USA

[3]Aryabhatta Research Institute of Observational Sciences, Nainital, India

[4]Center for Global and Regional Environmental Research, University of Iowa, Iowa City, IA 52242, USA

[5]Climate Service Center, Helmholtz Zentrum Geesthacht, Hamburg, Germany

Correspondence to: Rajesh Kumar (rkumar@ucar.edu)

This supplementary material contains text, two equations and two figures.

S1 Update of the F-TUV photolysis scheme

Here, we first examine the differences in aerosol optical properties due to use of different calculation methods in the optical driver and the F-TUV photolysis scheme. The impact of these differences on the distributions of photolysis rates and, surface ozone and NO_2 are described thereafter. The spatial distributions of aerosol optical depth (AOD), single scattering albedo (SSA) and asymmetry parameter (g) calculated by the F-TUV scheme and the optical driver at 300 nm are shown in Figure 1 for 21 April 2010 at 08 GMT to highlight the difference between the two schemes. Since the effect of dust aerosols is not included in the F-TUV scheme, we excluded their effect also from the optical driver for comparison in Figure S1. Both methods (F-TUV scheme and optical driver) yield similar spatial distributions of AOD over the model domain with highest values over the Indo-Gangetic Plain region, Himalayan foothills and northern Bay of Bengal, but differences in AOD between the two schemes range from -30% to 10%. Both the methods also show nearly similar spatial distributions for SSA and g with less spatial variability but there are large differences in SSA (30-50%) whereas the differences in g are within 10%. The analysis of spectral variations of SSA and g values used by the two methods for different aerosol components (black carbon, organic carbon, sulphate and sea-salt) suggested that the aforementioned differences in aerosol optical properties arise mainly due to differences in the optical properties of black carbon aerosols used by the two methods. The SSA values for BC aerosol used by the F-TUV scheme and optical driver in 300-736 nm wavelength range (representing the range of photolysis occurrence in the troposphere) are in the range of 0.08-0.14 and 0.03-0.21 respectively while the g values are in the range of 0.04-0.20 and 0.02-0.11 respectively. Both the methods use the SSA values of 0.98-1.0 for organic carbon, sulphate and

1   sea-salt aerosols, however there are differences in the g values of these aerosols between the two

2   methods particularly in the wavelength range of 447-736 nm.

3

4   To understand the importance of these differences in the context of gas-phase chemistry, we

5   coupled the aerosol optical properties calculated by the optical driver into the F-TUV photolysis

6   scheme. This coupling required the mapping of optical driver output at 4 wavelengths (300, 400,

7   600 and 999 nm) to 17 wavelengths (178-736 nm) of the F-TUV scheme. The AOD value at

8   each F-TUV wavelength is calculated following the Angström power law:

$$F(\lambda) = O(400) \times \left(\frac{\lambda}{400}\right)^{-\alpha} \tag{S1}$$

9   where F (λ) is the F-TUV AOD at wavelength λ (178-736 nm), O(400) is the AOD calculated by

10   the optical driver at 400 nm, and α is the Angström exponent calculated from optical driver's

11   AOD at 300 and 999 nm using the following relation:

$$\alpha = \frac{\ln\left(\frac{O(300)}{O(999)}\right)}{\ln\left(\frac{999}{300}\right)} \tag{S2}$$

12   The SSA and g values at each F-TUV wavelength are determined by linearly interpolating/

13   extrapolating the SSA and g values from the optical driver. This is the same method as is used by

14   the WRF-Chem to map the optical driver output to Rapid Radiative Transfer Model (RRTM)

15   spectra for calculating the effect of aerosols on meteorology.

16

17   The spatial distributions of NO_2 photolysis rate calculated using aerosol optical properties from

18   the F-TUV scheme and the optical driver on 21 April 2010 at 08 UTC are shown in Figure S2.

19   The spatial distributions of surface NO_2 and ozone are also shown to illustrate the impact of

20   differences in aerosol optical properties on simulation of key trace gases. The percentage

1   differences between the two methods are also shown. The NO_2 photolysis rates in both the

2   methods show similar spatial distributions with higher values over the oceanic regions and lower

3   over the inland regions. The lowest photolysis rates and highest differences (10-30%) are seen

4   along the Indo-Gangetic Plain region which is where the aerosol loading is highest (Figure S1).

5   Both NO_2 and ozone mixing ratios also show similar spatial distributions with highest values as

6   well as differences along the Indo-Gangetic Plain region. The differences are of the order of 3-

7   10% for NO_2 and 1-5% for ozone. These differences point out the inconsistency in the effects of

8   aerosols on gas phase chemistry in the WRF-Chem model. To avoid this inconsistency, we use

9   the aerosol optical properties from the optical driver to affect the photolysis rates as well as the

10   meteorology. This is because the SSA value simulated by the optical driver (0.8-0.9) are more

11   close to the measured value (0.75-0.9) reported for the Indian region (Ganguly et al., 2005) as

12   compared to the SSA simulated by the F-TUV scheme (0.5-0.6).

13
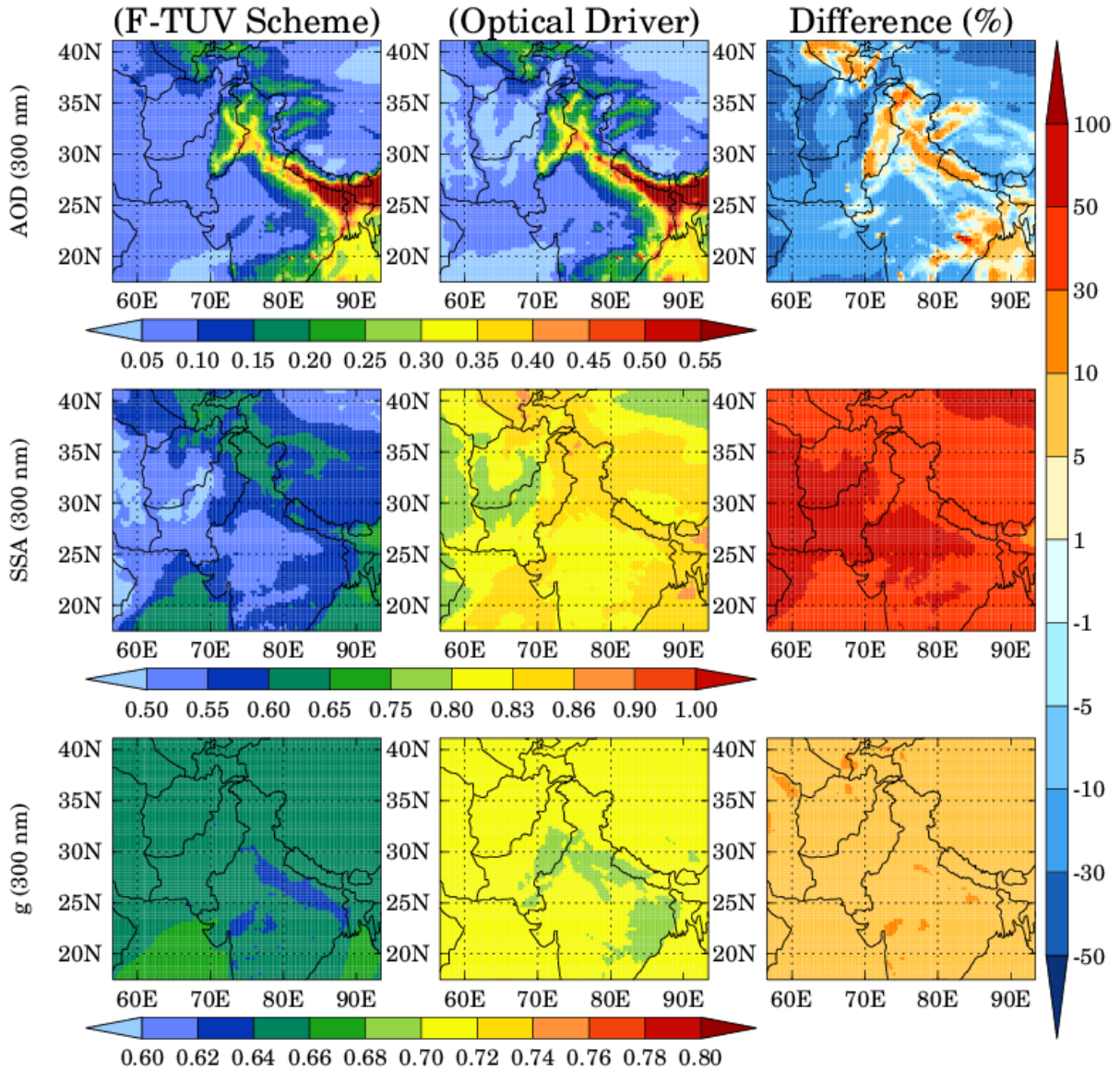
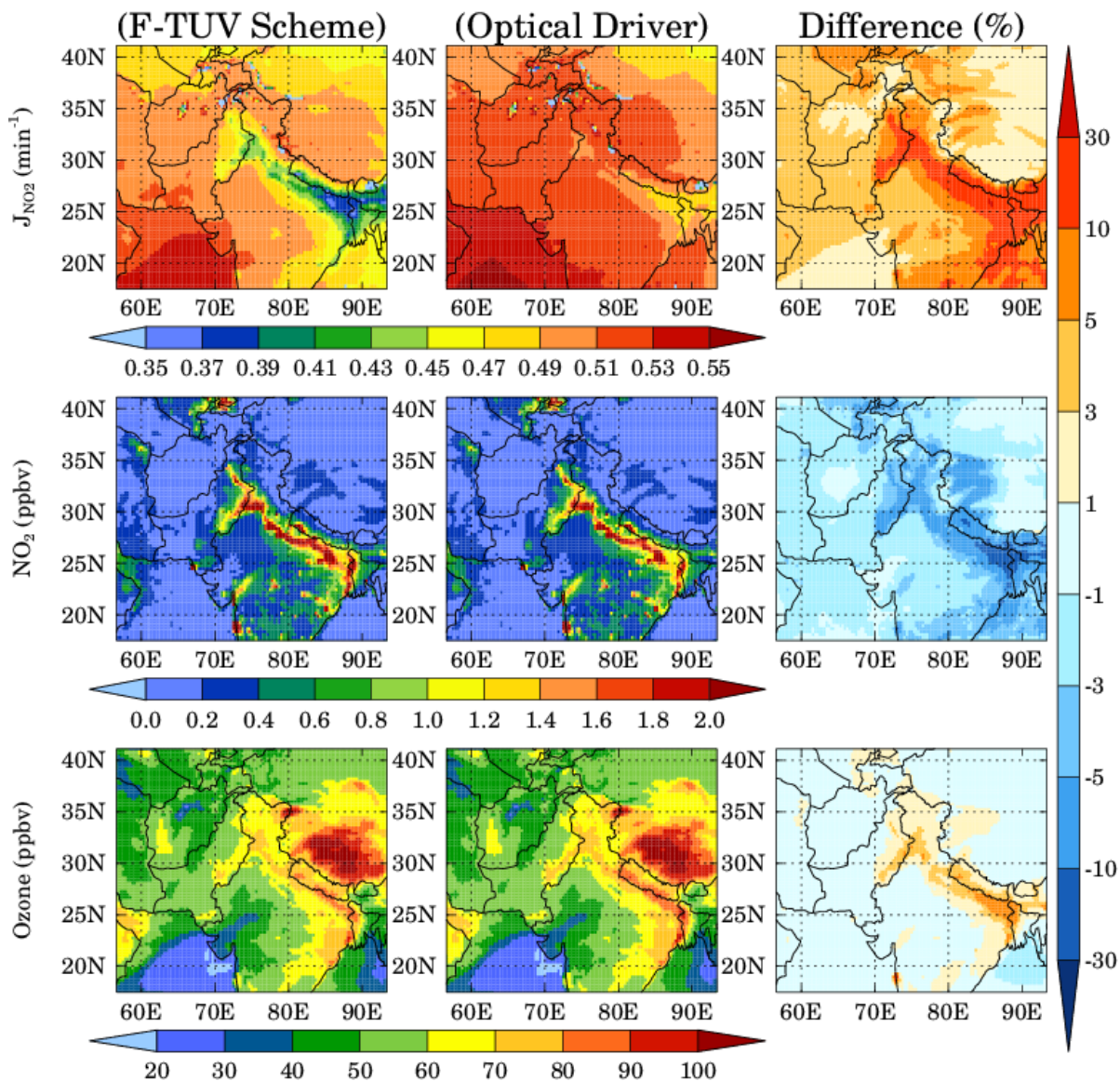**Figure S1:** Spatial distributions of aerosol optical depth (AOD), single scattering albedo (SSA) and asymmetry parameter (g) calculated by the F-TUV scheme and optical driver at 300 nm on 21 April 2010 at 08 GMT. The percentage differences in aerosol optical properties between F-TUV and optical driver are also shown.

Figure S2: Spatial distributions of NO$_2$ photolysis rate (J$_{NO2}$), NO$_2$ (ppbv) and ozone (ppbv) simulated by WRF-Chem using aerosol optical properties calculated by the F-TUV scheme and the optical driver on 21 April 2010 at 08 GMT. The percentage differences in all the parameters are also shown.